ELSEVIER

Electrically Induced Microstructural Changes in Portland Cement Pastes

Donggy Sohn and Thomas O. Mason
Northwestern University, Center for Advanced Cement Based Materials, Department of Materials Science and Engineering, Evanston, Illinois, USA

Portland cement pastes 1 day to 1 month old were each subjected to a single cycle of 1250 V/m electric field (15 s forward, 15 s off, 15 s reverse) and analyzed for microstructural/transport changes by impedance spectroscopy. All samples experienced an irreversible increase in resistance, as much as 20–25%, which decreased with increasing age of the paste. Subsequent applications of field produced no additional changes. The resistance increases were shown to be attributable to decreases in pore network connectivity rather than to changes in overall degree of hydration, capillary porosity, or pore fluid conductivity. It is proposed that electro-osmotic swelling of product near "bottleneck" pores results in the decreased connectivity. Ramifications for electrocuring, electromigration, electrochemical chloride treatment, and permeability studies of cement based products and structures are also discussed. Advanced Cement Based Materials 1998, 7, 81–88.
KEY WORDS: Cement paste, Electro-osmosis, Impedance spectroscopy, Pore structure

Large electrical fields have been shown to be useful in the processing, the characterization, and even the rehabilitation of cement based products and structures. For the purposes of this discussion, we will consider electric fields in excess of 100 V/m to be "large." *Electrocuring* [1, 2], which involves the use of ohmic heating to accelerate hydration, is energy efficient and allows for precise control of the curing cycle. High early strengths can be achieved. Fields of 300–500 V/m (usually A.C.) are required, according to Bredenkamp et al. [2]. In *electromigration*, large D.C. fields are used to drive ions through concrete [3]. The amount of current passed through a standard sample (cylinders of fixed area and thickness) in a set period of time is a measure of the conductivity/diffusivity. This is the basis of both AASHTO [4] and ASTM [5] "rapid chloride penetration" tests of concrete durability. Fields of 1180 V/m are maintained in such tests for 6 hours. *Electrochemical chloride removal* involves the use of large D.C. fields to drive unwanted chloride ions away from the steel reinforcement toward a temporary counter electrode on the surface. For example, fields of 100–1000 V/m were used in work of Tritthart et al. [6] and Tritthart [7]. Except for the recognition that excessive currents in electrocuring, electromigration, or electrochemical chloride treatments can cause Joule heating and be deleterious to the microstructure of concrete (cracking), none of the studies cited considered the effects of high applied field (and current density) on the underlying cement paste pore structure.

The observation of a strong electromechanical response in hardened cement pastes by Wittmann [8, 9], recently confirmed by Li et al. [10] and Yuan et al. [11], attests to the fact that substantial microstructural changes can occur in hardened pastes under applied field. There were detectable macroscopic (bending) deflections of a cement bar when fields of 6–40 kV/m were applied across its mid-section [8]. Expansive strains as large as 0.03% were observed under field strengths of ~50 kV/m [10]. These electromechanical effects were observed only when sufficient water was present. Both groups attributed the response to local swelling associated with a saturation gradient arising from electro-osmotic water transport in the direction of the applied field. Field reversal studies showed that some, but not all, of the deformation was reversible [11]. The reversible component was attributed to short-range redistribution of water within the specimen, and the irreversible component was attributed to long-range water transport towards the surface, as evidenced by expelled water droplets appearing on the surface.

Electrokinetic phenomena, such as electro-osmosis, occur in fine capillaries [12]. When an axial pressure gradient is imposed on an electrolyte in a capillary and the electrical current is restricted, an electric potential difference results between the ends of the tube. Conversely, when an axial electric field is applied to the electrolyte in the tube and the flow is restricted, a pressure difference appears between the ends of the tube. Electrokinetic phenomena require the formation

Address correspondence to: Dr. Thomas O. Mason, Northwestern University, Department of Materials Science and Engineering, 3037 Materials Life Science Building, Evanston, Illinois 60208.
Received July 28, 1997; Accepted September 29, 1997

ISSN 1065-7355/98/$19.00
PII S1065-7355(97)00056-4

of a diffuse charge layer in the electrolyte adjacent to the fixed surface charge on the capillary surface. An applied pressure forces fluid through the tube and imparts a finite velocity to the diffuse charge layer, resulting in an electrical potential difference along the tube. Conversely, a current flow through the tube results in fluid transport leading to a pressure differential along the tube. Morrison and Osterle [12] estimated a maximum electrokinetic energy conversion in glass capillaries with radii ~100 nm. This is comparable to the critical pore diameters typically obtained by mercury intrusion porosimetry of cement pastes. On the other hand, Yuan et al. [11] observed large, electrically induced strains in porous silica gels with pores ~ 25 Å. Silica gels with ~ 50 Å pore size had an order-of-magnitude smaller electrochemical response. These results suggest that the gel pores, rather than capillary pores, are responsible for the electromechanical response of cement based systems.

Impedance spectroscopy (IS) has been proven to be a relatively sensitive probe of the capillary pore structure of saturated cement pates [13]. The bulk conductivity is governed by the amount of capillary porosity, its conductivity (pore fluid conductivity), and its connectivity. In the present study, large fields (1250 V/m) of short duration (30 s total) were used to alter the microstructure of young cement pastes (28 days old or less), as determined by impedance based transport measurements. These results can be interpreted in terms of electro-osmotic swelling in the gel phase adjacent to constrictions in the capillary pore structure (i.e., "bottleneck" pores). Ramifications for the application of large fields in electrocuring, electromigration (e.g., rapid chloride penetration tests), and electrochemical chloride removal are considered.

Experimental Procedure

Type I Portland cement (La Farge) and deionized water were mixed using a kitchen blender at maximum speed for 5 minutes with a water-to-cement ratio of 0.4 by weight in all experiments. Pastes were cast into cylindrical plastic containers 5 cm in diameter and 8 cm long, with embedded stainless steel electrodes at each end. The specimens were vibrated to eliminate air bubbles, sealed, and stored at room temperature under 100% RH until testing.

Electric field experiments were carried out at 1, 3, 7, 14, or 28 days of hydration. In each case, a D.C. field of 1250 V/m was applied first in one direction for 15 s, then turned off for 15 s, and finally applied in the reverse direction for 15 s. At each hydration age, five separate samples were tested to allow for statistical analysis. Impedance measurements were conducted just prior to and immediately following the electric field treatment, and subsequently until steady state was achieved. A Hewlett-Packard 4192A impedance analyzer was used to collect data from 11 MHz to 5 Hz at 20 points per decade. Raw data were corrected using standard open- and closed-circuit nulling procedures outlined elsewhere [14]. The "Equivalent Circuit" fitting/simulation software package [15] was used to ascertain the specimen resistance at the cusp between the bulk and electrode arcs in each Nyquist (-imaginary vs. real impedance) plot. The resistance was converted to conductivity using the appropriate geometric factors.

It was important to ascertain whether detectable changes in pore fluid ion concentration (and conductivity) and/or in degree of hydration were taking place during the application of electric field. Within 10 to 20 minutes of electric field application and IS testing, samples were demolded and immediately subjected to crushing and pore fluid extraction using the die press described previously [16]. Pore fluid was captured in 10-ml syringes that were sealed until testing. Pore fluid conductivity was measured with the same impedance analyzer as used in the paste IS studies; a pH meter was used to determine the pH of each solution. Loss-on-ignition (LOI) was performed on portions of each specimen to determine the degree of hydration (α). Ground paste portion were weighed after 24 hours at 105°C and subsequently after 1000°C for 3 hours. The degree of hydration was calculated according to:

$$\alpha = [Wt(105°C) - Wt(1000°C)]/[0.24*Wt(1000°C)] \quad (1)$$

and was corrected for the degree of hydration of the dry cement (see [14, 17]). The capillary porosity of each paste was calculated from α using the Powers-Brownyard model (see [14, 18]):

$$\Phi(cap) = 1 - [(1 + 1.3\alpha)/(1 + 3.2\ w/c)] \quad (2)$$

where $w/c = 0.4$ in the present study. For selected specimens, an insulated type K thermocouple was embedded in the samples to determine the amount of temperature rise due to Joule heating.

Results and Analysis

Typical Nyquist plots of 7- and 28-day specimens before and after the application of field are shown in Figures 1A and 1B, respectively. Each specimen consists of a bulk arc at high frequencies and a spur at low frequencies. The spur is the beginning of a much larger arc associated with the steel electrode. The true sample resistance is found at the cusp between the electrode spur and the bulk arc. It can be seen that the sample resistance increases significantly with the application of

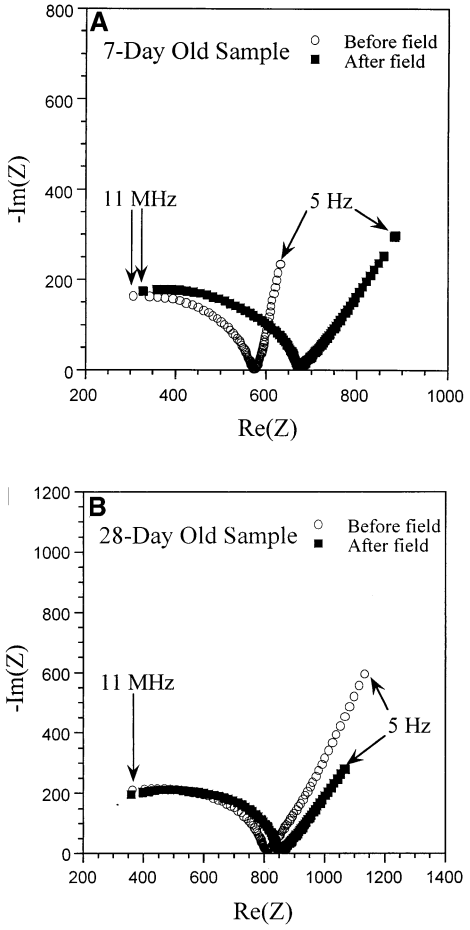

FIGURE 1. Nyquist plots of impedance data for OPC pastes with w/c = 0.4 before and after one cycle of 1250 V/m electric field (30 s duration, see text) on pastes pre-aged for (A) 7 days and (B) 28 days.

field for the 7-day sample, but much less so for the 28-day sample. Figure 2 shows that the fractional increase in resistance with the application of field vs. sample age. The error bars indicate the standard deviation of the five specimens tested at each age. Young pastes (<7 days) experience approximately 20–25% increases in resistance, whereafter the percentage increase falls off considerably. For example, the 28-day samples exhibit only 1–3% increases in resistance.

It was discovered that such permanent changes in sample resistance were only seen with the first cycle of electric field. The resistance changes with initial, second, and third cycles of electric field (1250 V/m) for a 3-day-old specimen are shown in Figure 3. Whereas the initial response was large and positive (21.4%), subsequent changes were much smaller and negative (−4.2%). Furthermore, whereas the initial resistance was never recovered after first application of field, the starting resistance for any subsequent application of field was recovered within 50–100 minutes.

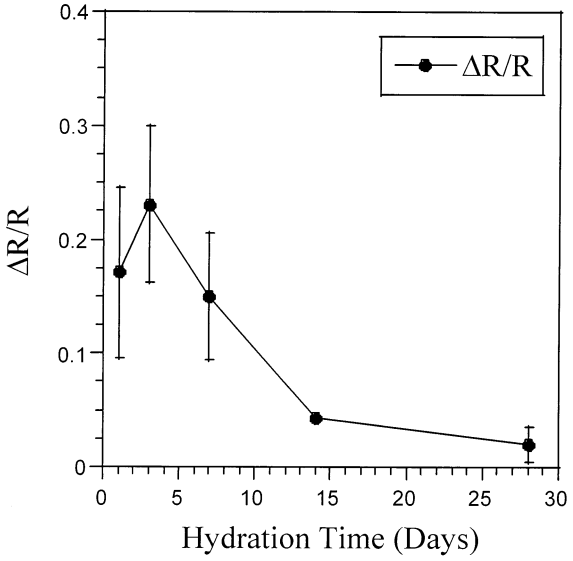

FIGURE 2. Fractional resistance change with one cycle of 1250 V/m electric field (30 s duration, see text) vs. time of hydration prior to test. The error bars indicate standard deviation on five samples.

The resistance drops associated with second and subsequent applications of field are due to Joule heating of the sample resulting in a slight increase in sample temperature. Based upon published values of heat capacity for hardened cement [19] and the total electrical power delivered to the sample in Figure 3, we estimate a temperature rise of 1.3–2.6°C. This assumes no heat loss to the environment. We can also estimate

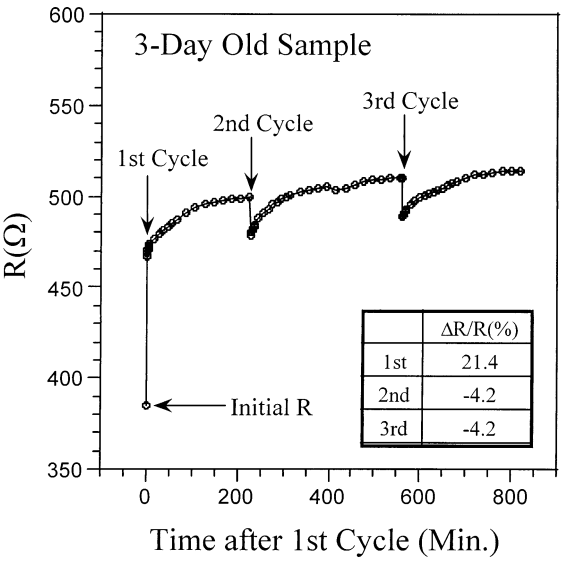

FIGURE 3. Resistance changes of 3-day-old specimen subjected to first, second, and third cycles of 1250 V/m electric field (30 s duration, see text).

Advn Cem Bas Mat
1998;7:81–88

the probable temperature change from the Arrhenius relationship for the pore fluid extracted from this sample:

$$\sigma_0 T = A \exp(-E_a/RT) \quad (3)$$

where E_a was determined to be ~ 13.1 kJ/mol. If only the pore fluid is considered and the contribution of all other phases are neglected, a 4% increase in conductivity would require an ~ 2.7°C increase in temperature. Actual thermocouple measurements before and after application of field indicated an increase of ~ 1.2°C. Therefore, we can account for the recoverable resistance drops associated with second and later applications of field. It should be stressed that a similar drop in resistance (increase in temperature) is also present in the first application of electric field; however, its influence is overwhelmed by the irreversible resistance increase observed. Once the sample subjected to a single application of field has thermally re-equilibrated with the ambient (50–100 min), the overall resistance increase is closer to 25.6%, the sum of the initial rise (21.4%), and the contrary 4.2% thermal effect.

A number of factors were considered to explain the large resistance rise on first application of field in Figures 1–3. Garboczi [20] introduced the following relationship for cement paste conductivity (σ):

$$\sigma = \sigma_0 \Phi_{cap} \beta \quad (4)$$

where σ_0 is the pore fluid conductivity, Φ_{cap} is the capillary porosity, and β is a "connectivity" parameter of the capillary pore network. Each of these three parameters could contribute to the overall irreversible change of resistance. The extracted pore fluid pH and conductivity before and after a single application of field are displayed vs. age of paste in Figures 4A and B, respectively. Again, the error bars represent the standard deviation from the measurements made on five samples at each age. The changes in pH are negligible. The changes in pore fluid conductivity, however, are significant. It should be pointed out that the changes at 1, 3, and 7 days are all in the wrong direction (*decreasing* resistance) to account for the irreversible *rise* in paste resistance with the first cycle of field. Based upon LOI data, the degree of hydration and corresponding capillary porosity were calculated before and after the first cycle. The results are shown in Figure 5. The changes observed are insignificant. Combining the data for pore fluid conductivity (Figure 4b) and capillary porosity (Figure 5), the connectivity parameter can be calculated from the experimental conductivities. These results are displayed in Figure 6. For young pastes (<14 days old) there are large reductions in pore phase connectivity, as much as 37%.

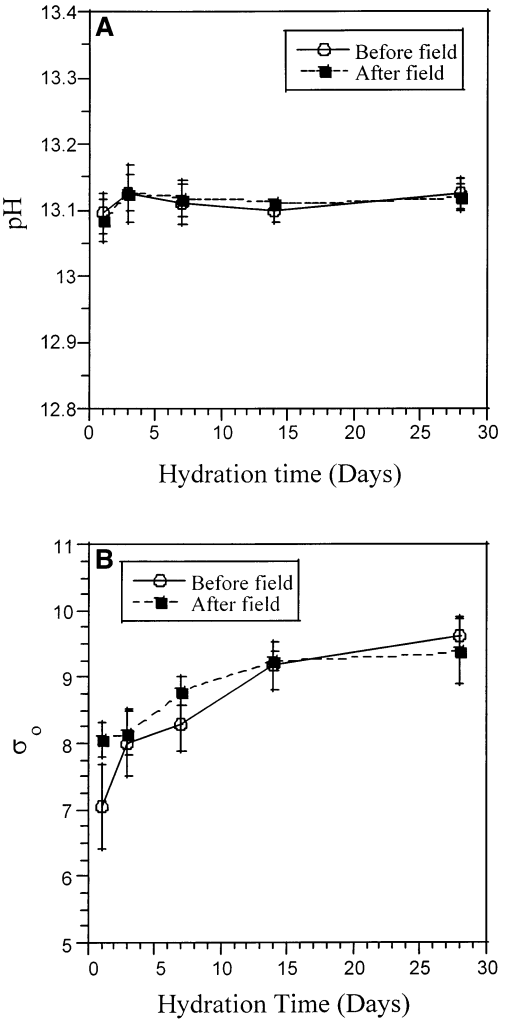

FIGURE 4. Pore fluid properties before and after the first cycle of 1250 V/m electric field (30 s duration, see text) as reflected in (A) pH and (B) electrical conductivity. The error bars indicate standard deviation on five samples.

Figure 2 suggests that older pastes are less susceptible to electrokinetic effects than are younger pastes. This is somewhat misleading, since paste resistance increases with age or degree of hydration. Younger pastes have significantly lower resistance and therefore experience much higher current densities for the same electric field strength.

To test for a current density-dependence of resistance change, 3-day-old samples were subjected to a range of electric field strengths. In Figure 7 the fractional change in sample resistance is plotted vs. current density. The field-induced change in resistance (and microstructure) increases with current density. Allowing for the significant sample-to-sample variability, as reflected in the error bars (the standard deviation of five samples), the fractional increase in resistance appears to be a linear function of current density. Also plotted in Figure 7 are

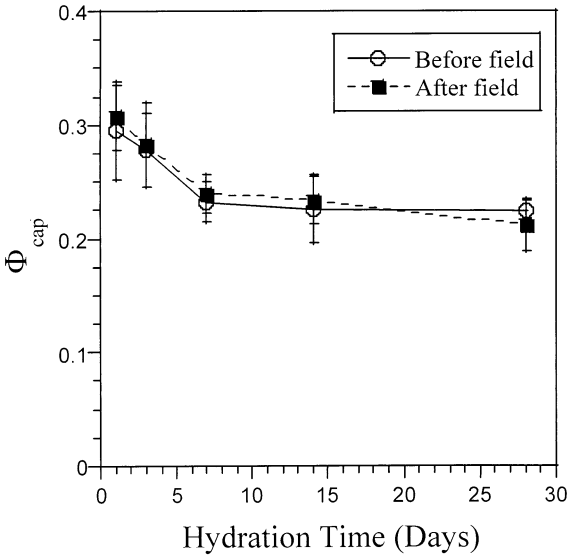

FIGURE 5. Capillary porosity vs. hydration age for samples before and after the first cycle of 1250 V/m electric field (30 s duration, see text).

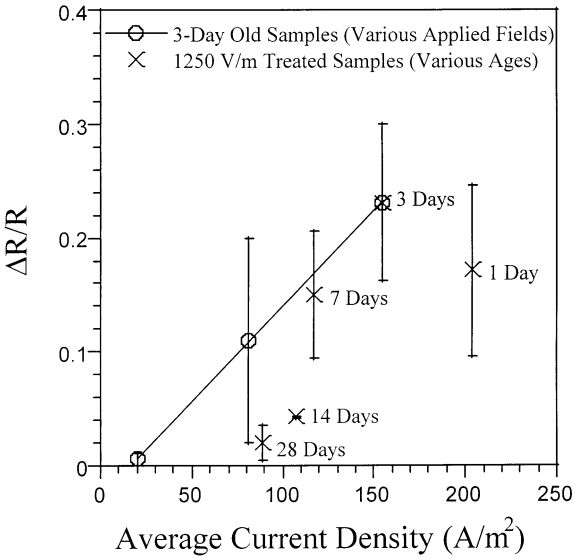

FIGURE 7. Fractional increase in resistance vs. overall current density used in the initial cycle of electric field (30 s duration, see text). The open points are for 3-day-old specimens at three levels of field (current density). The "Xs" are for the 1250 V/m treated specimens at the five ages shown in Figure 2. In each case, the error bars indicate the standard deviation of five specimens.

the fractional changes in resistance vs. current density for the original 1250 V/m test specimens. (The five values of current density correspond, in reverse order, to the five ages tested.) The early age (1-, 3-, and 7-day-old) specimens fall on or close to the 3-day-old ΔR/R vs. current density line, but the older pastes (14- and 28-day-old) fall significantly below it. This suggests that older pastes are less susceptible to electro-osmotic effects. On the other hand, some changes are registered at all ages, indicating that comparable microstructural modifications might result if sufficient current density is passed, the upper bound being the current at which the dielectric breakdown strength of the paste is exceeded.

Another interesting aspect of Figure 7 is that there may be a threshold current density below which little or no microstructural change is observed. A similar voltage (current density) threshold was reported in the electrochemical studies of Wittmann [8].

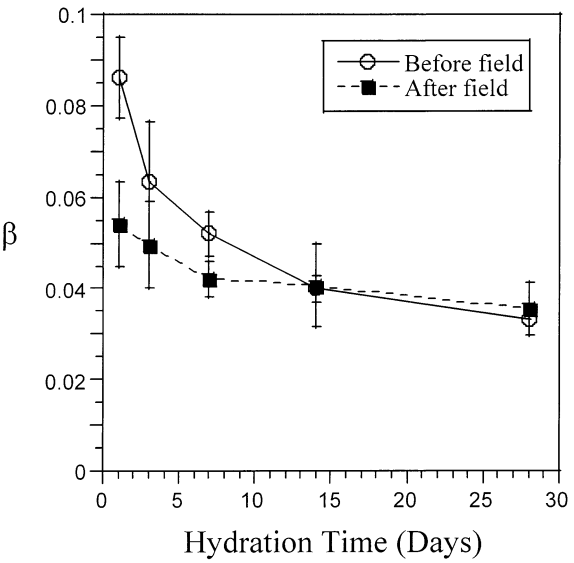

FIGURE 6. Connectivity parameter vs. hydration age for samples before and after the first cycle of 1250 V/m electric field (30 s duration, see text).

Discussion

The fact that little or no detectable change in overall degree of hydration or capillary porosity occurred upon application of field suggests that the irreversible increases in paste resistance (Figure 2) are attributable primarily to changes in the connectivity of the capillary pore phase (Figure 6). Figure 8 shows a schematic diagram of two adjacent capillary pores separated by a product layer with smaller "constriction" or "bottleneck" pores connecting them, one of which is pictured at the right. The conceptual model is supported by the microscopy study of Bonen and Diamond [21], who described the "groundmass" of cement paste as consisting of "cellular" or "skeletal" high-aspect-ratio ribs separating large capillary pores. The model is also consistent with the large dielectric constants obtained

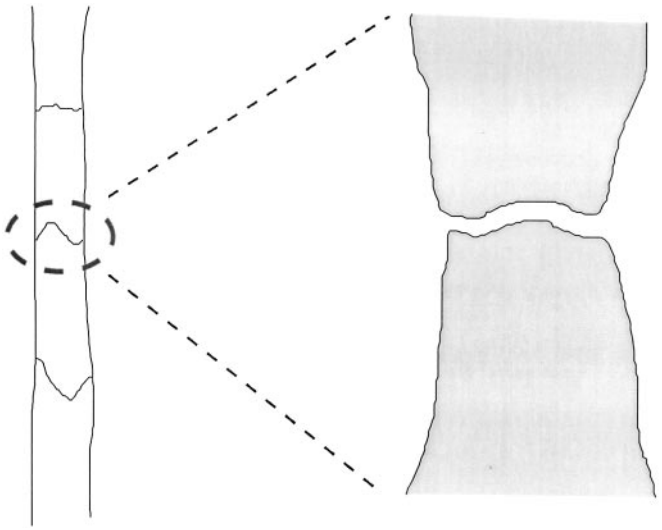

FIGURE 8. Schematic diagram of a C-S-H product layer separating adjoining capillary pores and a blow-up of a "bottleneck" pore connecting them.

for young cement pastes, where permeable, but tortuous, product barrier layers act as thin capacitors between adjacent capillary pores [22]. By narrowing or blocking the bottleneck pores, the connectivity parameter can be altered without significant changes in the overall porosity or degree of hydration. We now consider several mechanism whereby this might be accomplished by the application of electrical field/current.

The hydration rate of cement increases with temperature. Joule heating effects on the order of 1.2°C were detected in applied field tests of 3-day-old paste samples in the present study. Given that the local current density will be much larger in bottleneck pores, it is conceivable that large temperature increases in the vicinity of such pores might result in accelerated hydration and constriction of these pores, while leaving the overall degree of hydration largely unchanged. On the other hand, Joule heating should increase with the square of the current density. Sample-to-sample variability is quite large in Figure 7, but a more-or-less linear relationship between fractional resistance change and current density is observed. It is also hard to rationalize why only the initial application of field induces a response and subsequent episodes with virtually identical current density do not (see Figure 3).

According to electrokinetic theory, the passage of current along a capillary tube induces an axial present gradient. The "bottleneck" pores detected by mercury intrusion porosimetry are often on the order of 100 nm, at optimal size for electrokinetic conversion efficiently as estimated by Morrison and Osterle [12]. The electro-osmotic pressure gradient along such a bottleneck pore could be sufficient to deform the product layers surrounding the pore. There would be a tendency to collapse the pore at its low pressure orifice, thereby resulting in a decrease in connectivity even if the opposing orifice is widened. In agreement with the results in Figure 7, the pressure gradient should vary linearly with electric field [12]. It is also conceivable that there is a threshold pressure gradient below which deformation is not possible. The only drawback with this model is that it fails to explain why episodes of electric field subsequent to the first result in no additional deformation.

The highest electric field gradients within the cement paste will occur at bottleneck pores. These gradient should vary linearly with the overall current density (and external applied field). Yuan et al. [11] observed large electromechanical responses, comparable to that of cement pastes, in silica gels with ~25 Å pores, whereas an order-of-magnitude smaller response was obtained for silica gels with ~50 Å pores. They concluded that the electrically induced strains they observed in cement pastes were due to water redistribution between gel pores or between gel pores and interlayer positions, giving rise to local swelling effects [11]. Given that the maximum local fields are in the vicinity of bottleneck pores, it makes sense that the first indications of C-S-H swelling would show up there. Although we have no means to estimate the local field strength at bottleneck pores in the present study, Yuan et al. [11] observed a threshold for field-induced mechanism deformation of between 25 and 50 kV/m in 2-month-old cement paste samples.

It is also interesting that Yuan et al. [11] observed irreversible and reversible electromechanical responses in cement pastes. The irreversible contribution was dominant in the first cycle of alternating field (at 0.01 Hz), but reduced considerably in later cycles and was virtually absent after the third cycle. They correlated the irreversible response to the appearance of water droplets on the surface of their samples and overall loss of water content, i.e., electro-osmotic water expulsion. Although we observed no water loss from the samples in the present study, there may be a correlation between the early (or first) cycle irreversibility in our two studies.

The precise mechanism for local expansion of C-S-H leading to constriction of bottleneck pores, and thereby a reduction in pore connectivity, remains an open question. Wittmann [23, 24] described hardened cement pastes as xerogels, i.e., the Munich model, whose particles could be separated (structural expansion) by a disjoining pressure upon water absorption. Feldman and Sereda [25], on the other hand, believed xerogel behavior to be controlled by addition of water in the interlayer positions rather than by capillary condensation. It is conceivable that electro-osmotically induced

redistribution of water between gel pores and interlayer positions could lead to irreversible deformations, whereas the redistribution of water among gel pores could produce reversible deformations, or vice versa. Regardless of the mechanism, the present results suggest that irreversible deformations take place in the vicinity of bottleneck pores upon the application of field, leading to a reduction in pore network connectivity.

The present study has important ramifications for the electrocuring, electromigration, and electrochemical chloride treatment of cement based materials and structures. Although these procedures use similar electric fields (100–1000 V/m), they involve much longer periods of application. This suggests that significant microstructural changes are possible during the test/procedure. This may actually be advantageous in electrocuring, if a higher resistance (less diffusible) and therefore more durable product results. An increase in resistance (due to decreased connectivity) could also be a side benefit of electrochemical chloride treatment of rebar-containing structures. In both cases it is imperative to limit Joule heating so as not to damage the microstructure due to cracking. The most troubling consequence of electro-osmosis is with respect to the standard AASHTO [4] and ASTM [5] tests for "rapid chloride penetration," which involve field application for up to 6 hours. It is quite conceivable, based upon the present results, that the microstructure (and diffusivity) of cement/concrete is continuously changing during the course of the experiment. These tests may be of limited value in establishing the actual diffusivity of a concrete specimen.

One final ramification of the current results has to do with standard hydraulic permeability measurements. The converse electrokinetic effect, i.e., the generation of a "streaming current" upon application of a pressure gradient, may play an important role. In other words, electro-osmotic swelling effects may also occur during permeability testing, where a substantial pressure gradient is used to force water through the cement/paste pore network. It is routinely observed that "equilibrium flow" requires up to 1 month to obtain, during which time the coefficient of permeability drops by as much as an order of magnitude [26]. Furthermore, it has been demonstrated that the coefficient of permeability decreases as the pressure head used for the test increases [27]. It is possible to account for both of these observations on the basis of electro-osmotic constriction of bottleneck pores. Higher pressure gradients (increased flow) would induce larger streaming currents. Banthia and Mindess [26] have espoused high pressure "conditioning" of specimens prior to hydraulic permeability measurements.

The sensitivity of the permeability coefficient to changes in bottleneck pores can be understood by the Katz-Thompson equation, originally developed for porous rocks [28]:

$$k_p = (1/226)d_c^2(\sigma/\sigma_0) \quad (5)$$

where k_p is the hydraulic permeability, (σ/σ_0) is the ratio of paste conductivity-to-pore fluid conductivity, and d_c is a "critical pore diameter" from mercury intrusion porosimetry. This pore diameter may well be something like the diameter of the largest bottleneck pores (see Figure 8). Since (σ/σ_0) also decreases with the bottleneck pore diameter (both vs. time and with first field in Figure 6), it is not surprising that the hydraulic permeability would be highly sensitive to electro-osmotic effects.

Acknowledgments

This work was supported by the National Science Foundation through the Science and Technology Center for Advanced Cement-Based Materials under grant no. DMR-91-20002. The authors are grateful to Professors Lynn Johnson and Hamlin Jennings and to Jin-Ha Hwang, John Shane, and Steve Ford for helpful discussions.

References

1. Orchard D.F.; Barnett, A.M. *J. Mater. JMLSA* **1971,** *6*, 617–642.
2. Bredenkamp, S.; Kruger, D.; Bredenkamp, G.L. *Mag. Concr. Res.* **1993,** *162*, 71–74.
3. Whiting, D. *Public Roads* **1981,** *45*, 101–112.
4. *AASHTO-T277-93*; American Association of State Highway Transportation Officials: Washington, DC.
5. *ASTM-C1202-94*; American Society for Testing and Materials: Philadelphia, PA.
6. Tritthart, J.; Pettersson, K.; Sorensen, B. *Cem. Concr. Res.* **1993,** *23*, 1095–1104.
7. Tritthart, J. In *Proceedings of the* 2nd *CANMET/ACI International Symposium*; Detroit, MI, 1995; p 127.
8. Wittmann, F.H. *Cem. Concr. Res.* **1973,** *3*, 601–605.
9. Wittmann, F.H.; Hollenz, C. *Cem. Concr. Res.* **1974,** *4*, 389–397.
10. Li, J.-F.; Ai, H.; Viehland, D. *J. Am. Ceram. Soc.* **1995,** *78*, 416–420.
11. Yuan, L.; Li, J.-F.; Viehland, D. *J. Am. Ceram. Soc.* **1995,** *78*, 3233–3243.
12. Morrison, F.A.; Osterle, J.F. *J. Chem. Phys.* **1965,** *43*, 2111–2115.
13. Christensen, B.J.; Coverdale, R.T.; Olson, R.A.; Ford, S.J.; Garboczi, E.J.; Jennings, H.M.; Mason, T.O. *J. Am. Ceram. Soc.* **1994,** *11*, 2789–2804.
14. Christensen, B.J.; *Ph.D. Thesis*; Northwestern University: Evanston, IL, 1993.
15. Boukamp, B.A. *Equivalent Circuit*; University of Twente: The Netherlands, 1988.
16. Barneyback, R.S.; Diamond, S. *Cem. Concr. Res.* **1981,** *11*, 279–285.
17. Mindess, S.; Young, J.F. *Concrete*; Prentice-Hall: Englewood Cliffs, NJ, 1981.

18. Taylor, H.F.W. *Cement Chemistry*; Academic Press: San Diego, CA, 1990.
19. Bazant, Z.P.; Kaplan, M.F. *Concrete at High Temperature: Material Properties and Mathematical Models*; Longman: Harlow, England, 1996.
20. Garboczi, E.J. *Cem. Concr. Res.* **1990,** *20*, 591–601.
21. Diamond, S.; Bonen, D. *J. Am. Ceram. Soc.* **1993,** *76*, 2993–2999.
22. Ford, S.J.; Hwang, J.-H.; Shane, J.D.; Olson, R.A.; Moss, G.M.; Jennings, H.M.; Mason, T.O. *Adv. Cem. Based Mat.* **1997,** *5*, 41–48.
23. Wittmann, F.H. *Proceedings of the Conference on Hydraulic Cement Pastes: Their Structure and Properties*; Sheffield, England, 1976, p 96.
24. Wittmann, F.H. *Deutsch. Ausschus. Stahlbeton* **1977,** *290*, 43–101.
25. Feldman, R.; Sereda, P. *Mater. Constr. (Paris)* **1968,** *1*, 509–520.
26. Banthia, N.; Mindess, S. *Cem. Concr. Res.* **1989,** *19*, 727–736.
27. Nyame, B.K.; Illston, J.M. *Mag. Concr. Res.* **1981,** *55*, 139–146.
28. Katz, A.J.; Thompson, A.H. *Phys. Rev. B* **1986,** *34*, 8179–8181.